Contribution into Robust Optimization of Renewable Energy Sources: Case Study of a Standalone Hybrid Renewable System in Cameroon

Wulfran FENDZI MBASSO *‡, Serge Raoul DZONDE NAOUSSI *,
Reagan Jean Jacques MOLU *, Saatong KENFACK TSOBZE **

* Technology and Applied Sciences Laboratory, U.I.T. of Douala, University of Douala, Cameroon, P.O. Box 8689 – Douala

** Unité de Recherche d'Automatique et d'Informatique Appliquée, I.U.T. Fotso Victor, University of Dschang, Cameroon, P.O. Box 134 – Bandjoun

(fendzi.wulfran@yahoo.fr, sdzonde@gmail.com, molureagan@yahoo.fr, saakenft@yahoo.fr)

‡ FENDZI MBASSO Wulfran; DZONDE NAOUSSI Serge Raoul; MOLU Reagan Jean Jacques; KENFACK TSOBZE Saatong, P.O. Box 8689 – Douala, Tel: +237 694 160 659,

Fax: +237 694 160 659, fendzi.wulfran@yahoo.fr

Received: 11.04.2023 Accepted:06.06.2023

Abstract- Environment conservation is a matter subject affecting both developing and developed countries. Long-lasting energy can be achieved by attenuating Greenhouse gas emissions. All over the world, Hybrid Renewable Energy Sources (HRES) appear as a vital element when it comes to cover the rapid growth of the energy demand. Moreover, renewable energy (RE) is an unaffordable response to the fight against unpredicted events such as the diseases, industries development, reliability of energy sources, added to the various directives related to produce sustainable electricity. Henceforth, it is crucial to optimize the various sources for satisfying the electrical demand. In particular, this paper aims to value the hybridization of optimization techniques to achieve a robust optimization. Photovoltaic (PV), and Battery Storage Systems (BSS) constitute the various RE sources in this work. The main goal was to simultaneously minimize the Deficit of power supply probability (DPSP) and maximize the BSS capacities. Particle Swarm Optimization (PSO), Grey Wolf Optimizer (GWO), and hybridization of both techniques are employed to proceed with the optimization. This study reveals the performance of hybrid optimization used for several configurations of loads. Indeed, the results show that the autonomous day of the BSS can reach 03 days, while the DPSP can decrease towards 1%. Hence, the obtained HRES is eco-friendlier and more autonomous. Furthermore, the proposed idea provides improved reliability and robustness of our system under various types of loads due to different climate scenario. A statistical analysis shows a good stability and better efficiency while doing hybridization of both techniques.

Keywords Deficit of power supply probability (DPSP), Hybrid Renewable Energy Sources (HRES), Autonomous days, Particle Swarm Optimization (PSO), Grey Wolf Optimizer (GWO) Hybrid Optimization, Robustness.

Abbreviations and Nomenclature

GHG	Green House Gas
HRES	Hybrid Renewable Energy Sources
IEA	International Energy Agency
COVID	Corona Virus Disease
RE	Renewable Energy
PV	Photovoltaic
RES	Renewable Energy Sources
HSA	Harmony Search Algorithm
JOA	Jaya Optimization Algorithm
PSO	Particle Swarm Optimization
COE	Cost Of Energy
LPSP	Deficit of power supply probability
EQ	Equilibrium Optimizer
BAT	Bat algorithm
BHB	Black-hole-based algorithm
RF	Renewable Factor
NPC	Net Present Cost
WT	Wind Turbine
BSS	Battery Storage Systems
HOMER	Hybrid Optimization of Multiple Energy Resources
TRNSYS	Transient System Simulation
PSO	Particle Swarm Optimization
DC	Direct Current
AC	Alternating Current
LIHR	Low Investment with High Rating
P_{PV}	Hourly power of the PV (kW)
P_r	Rated power of the PV (kW)
G_{ref}	Reference solar radiation (1kW/m²)
G	Solar radiation (W/m²)
f_v	Derating factor of the PV
T_{ref}	Reference temperature of the cell (◦C)
K_T	Temperature coefficient (/◦C)
T_C	Temperature of the cell (°C)
T_{amb}	Ambient temperature (◦C)
NASA	National Aeronautics and Space Administration
η_{inv}	Efficiency of the inverter
P_{in}	Input power of the inverter (kW)
DOD	Depth Of Discharge
SOC	State Of Charge
P_{ch}	Instantaneous power of the battery at the charging (kW)
P_{disch}	Instantaneous power of the battery at the discharging (kW)
η_{ch}	Efficiency of the battery at the charging
η_{disch}	Efficiency of the battery at the discharging
SOC (t)	State of charge of the battery at t
SOC (t-1)	State of charge of the battery at t-1
σ	Self-discharge factor of a battery
AD	Autonomous days of the battery
P_{BSS}	Hourly power of the BSS (kW)
P_L	Hourly power of the load (kW)
$P_{bat\,min}$	Minimum allowable battery power (kW)
$P_{bat\,max}$	Maximum allowable battery power (kW)
GWO	Grey Wolf Optimizer
E_{dumped}	Energy dumped (stored) into the battery (kWh)
AD_{min}	Minimum autonomous days of the HRES
AD_{max}	Maximum autonomous days of the HRES
LPS	Loss of Power Supply
q	Maximization function for the system
λ_1	Weighing factor of the AD
λ_2	Weighing factor of the E_{dumped}
RF	Renewable Factor
P_{RE}	Hourly power provided by the PV module and the battery storage system (kW)
β_L	Reliability limit tolerance
SOC_{min}	Minimum value for state of charge
SOC_{max}	Maximum value for state of charge
P_{PV}	Hourly power of the PV (kW)

x_k^i	Position of the i-particle at iteration k
v_k^i	Velocity of the i-particle at iteration k
x_{k+1}^i	Position of the i-particle at iteration k+1
v_{k+1}^i	Velocity of the i-particle at iteration k+1
p^i	Best individual particle position
p^g	Best global position
c_1	Cognitive parameter
c_2	Social parameter
r_1	Real within interval 0 and 1
r_2	Real within interval 0 and 1
$\vec{C}$	Coefficient vector
$\vec{Q}$	Coefficient vector
x_p	Vector for the prey's position
$\vec{D}$	Vector for the wolf's position
Y_{min}	Best value for the applied technique
n_{sim}	Total number of simulations
η_{bat}	Efficiency of the battery
$\vec{r}$	Vector of components
a_1	Real within interval 0 and 1
a_2	Real within interval 0 and 1
MOO	Multi Objective Optimization
MOPSO	Multi Objective Particle Swarm Optimization
SOO	Single Objective Optimization
DSM	Demand Side Management
MAE	Mean Absolute Error
SD	Standard Deviation
RMSE	Root Mean Square Error
RE	Relative Error
E_{disch}	Energy of the battery at discharging (kWh)
E_{ch}	Energy of the battery at charging (kWh)
Y_β	Second best position in each iteration
Y_δ	Third best position in each iteration
$\vec{C}$	Coefficient vector
$\vec{Q}$	Coefficient vector
x_p	Vector indicating the position of the prey
$\vec{D}$	Vector indicating the position wolf
Y_i	Position for the applied technique at each simulation.
α	Leading grey wolf
β	Superior grey wolf
δ	Medium grey wolf
ω	Inferior grey wolf
$\vec{W}_\alpha$	Mathematical model of wolf α
$\vec{W}_\beta$	Mathematical model of wolf β
$\vec{W}_\delta$	Mathematical model of wolf δ
chi1	Random real value between 0 and 1 for PSO
chi2	Random real value between 0 and 1 for PSO
A_1	Coefficient vector for wolf α
A_2	Coefficient vector for wolf β
A_3	Coefficient vector for wolf δ
Q_1	Coefficient vector for the first best position in each iteration
Q_2	Coefficient vector for the second best position in each iteration
Q_3	Coefficient vector for the third best position in each iteration
$c_1 r_1 (p_k^i - x_k^i)$	Cognitive component of each particle at each iteration
$c_2 r_2 (p_k^g - x_k^i)$	Social component of each particle at each iteration

1. Introduction

Nowadays, energy is crucial for every society at any stage and every sector. The different sources of energy employed and the tracking for the development imply deploying advanced modern technologies with both positive and negative impacts. An undeniable consequence of this issue is the drastic change of the world climate leading to environmental alterations [1]. Scholars found in Renewable Energy Sources (RES) a lasting solution to preserve the environment and improve stability, energy security, and sustainable power generation [2]. Nonetheless, the inconsistent output of these sources leads to the use of more than one of them to constitute a Hybrid Renewable Energy System (HRES). Several works have revealed the benefits of HRES in terms of efficiency and costs [3…5]. For distant localities including agricultural farms, petroleum platforms, and islands…., their use is a strength as they offer more reliability in their operation.

However, about 800 million people in several countries in Africa and Asia will still not have access to electricity for the next decades [6…7]. This results into an increase of energy consumption of more than 50% by 2035 worldwide to cover [8]. Developing countries need to shift to eco-friendly power for the following benefits: health and employment improvement, carbon footprint reduction; etc. This is also a concern for Cameroon whose energy consumption will grow in an unparallel rate [9]. In the same idea of improving the energy sector with the different projects launched by the government in the country, this work will carry proper investigation to reveal the advantages of the penetration of renewable energy into energy sector of the country. This will enable the growth of RE usage which is evaluated at just 1% of the total electricity production [10].

1.1. Literature Review

For decades, the world is under perpetual alterations in all domains: social, economic, environmental, health…. Many factors have contributed to these significant changes. COVID-19, for instance, has affected the energy consumption worldwide [11], with positive impact on the environment due to pollution reduction. The transition to sustainable sources of energy is unavoidable and various combinations of energy sources are used to fulfil the first requirement: cover the demand [12…14]. The variability of RES conducts into using one or more energy sources to obtain HRES and assess them for several reasons. [15] used various energy sources to determine the optimal configuration. Three different algorithms namely Harmony search algorithm (HSA), Jaya optimization algorithm (JOA) and Particle swarm optimization (PSO) are employed to fulfil two objectives: minimize the cost of energy (COE) and determine the minimum limit value of the deficit of power supply probability (DPSP). The results obtained show an optimal system with a least cost and an improved reliability. Indeed, the ideal solution comprises in thirteen PV, four biomass systems, one wind turbine and fifteen BSS, for a total present cost of \$581,218 and a cost of energy of 0.254 \$/kWh. Furthermore, scholars in [16] have investigated on the impact of Soot on the efficiency of solar panels. Using a Smart Intelligent Monitoring System, results have shown an improvement of the efficiency of the solar panels integrated into the HRES.

Likewise, HRES associated with storage systems are more profitable than those without. Authors [17] have obtained a convenable solution to the problem of standalone cities in Southern Nigeria, a technical analysis has been performed. Results show that the equilibrium demand-supply has been satisfied with the HRES employed. Besides, [18] have proposed a methodology to optimize a hybrid PV-storage system grid connected. In this paper, authors revealed the benefit of integrating BSS into HRES such as reducing the COE purchased from the grid and cover the gap due to the sporadic nature of RES. In another work, [19] proposed an optimal planification of energy storage for power systems in short-term previsions. In addition to the cost-effectiveness, many authors have enumerated other benefits of HRES combined with storage systems, namely: reliability, load satisfaction and ecofriendly. [20] has employed many evolutionary algorithms to build up an optimal autonomous HRES. Authors have minimized the DPSP to improve the reliability of the system. In [21], a review has been elaborated a review on HRES by characterizing their optimal size, the control, and the management strategies. In this paper, a deep analysis has been drawn to reduce the cost function from the optimal model. [22] proposed an optimal HRES in an off-grid HRES taking into consideration the following aspects: economic and environmental parameters. In this work, the results show a COE of 0.691 (USD/kWh) and an annual emission of CO_2 of only 4.43 kg. The proposed system shows an improvement of 18% of the net present cost (NPC) compared to the existing microgrid, and an ecofriendly system with a reduction of emissions of greenhouse gas.

In recent years, many works reported optimum sizes of HRES using various optimization algorithms. For single or multi-objectives, the purposes remain mainly into minimizing cost and improving system's reliability [23…26]. In [27], a techno economic analysis and optimization are realized into a HRES comprised of PV, WT, and BSS for a community in Saudi Arabia.

Besides, alone [28…29] or combined with other methods [30…32] such as modern technologies and programming softwares like Hybrid Optimization of Multiple Energy Resources (HOMER), Transient System Simulation Tool (TRNSYS)…, optimization algorithms have proved their ability to obtain good results into optimization process. In addition, many studies are based under uncertainty in two parts: from the sporadic nature of the loads and from the variability of RES. In both cases, optimization is characterized as robust, and the results are more accurate. This study argues on the use of hybrid optimization algorithms as an important step into robust optimization. The case study is described as some households in a sub-Saharan country.

1.2. Research Gap and Contributions

Each society needs electricity to ensure its development in several domains: social, economy…[33]. Many African countries are highly affected by the lack of electricity, especially in sub-Saharan countries. Cameroon is rated at about 65% of electrification ratio, a value above most African countries which rate is at 48% [34]. In rural communities, more than 80% of the population are not electrified [35]. Surprisingly, these parts of the country abound with infinite renewable energy resources like solar energy resource in the northern part, wind in the western and coastal areas. Moreover, the HRES are not grid connected and henceforth, many studies are based on standalone systems. For instance, this work aims to:

- Emphasize on utilizing RES in electricity sector as a lasting response to various changes; indeed, our HRES consists of PV/BSS
- Enhance the proliferation of micro grid into rural communities of Cameroon, as RES are not yet connected to the main power supplier.
- Contribute into valuing robust optimization of HRES with hybridization of optimization algorithms, especially when using various seasons or different configurations of loads.

Furthermore, the study case is the Littoral region of Cameroon, a coastal area in the country. Henceforth, the analysis carried out has the main goal to maximize the autonomy of the HRES through the energy stored and the autonomous days, but more important to ameliorate the reliability of the system by minimizing the DPSP.

1.3. Paper Structure

A thorough methodology is performed in this paper as per the following organization: In section 2, the modelling of our HRES is presented. Section 3 formulates the problem by developing the energy management strategy, and the various functions (objective and constraints) employed for the optimization. Section 4 depicts the different optimization techniques used in this paper. Further, the results of the simulations performed are presented in section 5, highlighting the performance of the applied algorithms. Ultimately, the conclusion of the paper is presented in the last section.

2. Mathematical Modelling of the HRES

To achieve the goal of covering the demands in terms of energy in some households in Cameroon, an optimization based on several criteria has been performed. Every hour, the power demand of every activity sector (hospital, school, trade …) is highlighted based on the actual electrical appliances currently found in these households; but also, on the two main seasons that are met in those areas, namely dry season, and rainy season. Henceforth, several multi criteria optimization has been performed in this paper.

This section describes the methodology for achieving our optimization as follows: (2.1) System modelling; (2.2) Meteorological data, (2.3) Load data, (2.4) The mathematical modelling of the HRES, and (2.5) Optimization problem formulation. Lastly, a detailed presentation of the hybrid optimization algorithm is realized. Then, power management strategies and various constraints of the HRES are investigated to obtain the optimal solutions of the problem. All the computations done in this paper are done every hour.

2.1. System Modelling

The designed HRES consists of four fundamental parts as shown in (Fig.1): PV Module, DC/AC Converter, Battery Storage systems, Electrical loads [36]. The power electronic converter used is suitable with the system power requirements.

2.2. Meteorological Data

In this section, the HRES will be presented from the load demand to the renewable energy sources.

2.2.1. Case Study

With an area of 475,442 km^2, Cameroon is ranked as the world's 53^{rd}-largest country. This country is located in Central and West Africa. Between longitudes 8° and 17°E and latitudes 1° and 13°N, Cameroon has a control on a part of the Atlantic Ocean (Fig. 2).

Known as the economic capital of the country, Douala, our focus area, is the largest city in Cameroon (Fig. 3). Located at 04°03′N 009°41′E, Douala subject to a tropical climate, with approximatively constant temperatures all over the year. But, during July and August, the town undergoes cooler temperatures. Douala experiments both hot and cool conditions, knowing an average annual temperature of 27.0 °C (80.6 °F) and an average humidity of 83% [37]. During the year, Douala encounters a lot of rainfall, experiencing on average roughly 3,600 millimeters (140 in) of precipitation per year [37]. Henceforth, the city is full of RES and renewable energy context can be explored in this locality.

In particular, our attention will be put on a specific location in Douala, Ndogbong (Fig. 4). Found at Latitude 4.06447° or 4° 3' 52" north and Longitude 9.75213° or 9° 45' 8" east, this suburb hosts population of all levels, depending on the life conditions. The study case is a household located at Ndogbong which load will rely on the meteorological data every hour.

2.2.2. Weather Data

(Fig. 5) presents the scales of the solar radiation of the country. For the concerned location, the data are gathered for a period of one year (8760 h). In (Fig. 6), 5.8 kW/m^2 is the minimum daily radiation, 6 kW/m^2 is the median value and 6.46 kW/m^2/day is the maximum daily radiation. Therefore, this region is suitable to install solar PV.

2.3. Load Data

For the case study, the load is made up of electrical equipment commonly used for household. For instance, we have fan, PC, TV, washing machine, heater, charger, iron, lamps, fridge which constitute Low Investment with High Rating Equipments [38]. This is justified by the actual living conditions of people in that location, with medium life standards. Four configurations of load are presented depending on the seasons and the number of devices in the household. Tables 1, 2, 3 and 4 depict the hourly energy consumption. In Figures 7a, 7b, 7c, and 7d, the various load variations show that there is no deviation, henceforth the load used for the study is realistic. During rainy season, the maximum power is 2.47kW for a great consumer and 1.47kW for a low consumer. In addition, the minimum consumption is 0.1kW and 0.06kW for a great consumer and a low consumer respectively. Similarly, during dry season, the maximum power is 2.47kW for a great consumer and 1.47kW for a low consumer. But the minimum consumption is 0.155kW and 0.065kW for a great consumer and a low consumer respectively.

Moreover, meteorological conditions and socio-economic factors can highly influence power supply. In [39], authors establish a dependent relation between load (hence electricity generation) and weather. Indeed, wind speed, humidity and temperature have a huge impact into human's life, henceforth into their consumption of electricity. This explains the fluctuation in terms of energy consumption in the considered load profile.

Thus, meeting the demand requires sustainable, and clean energy sources. Nevertheless, in Cameroon, renewable energy is not yet well distinct. This work proposes a reliable HRES to work under various meteorological uncertainties.

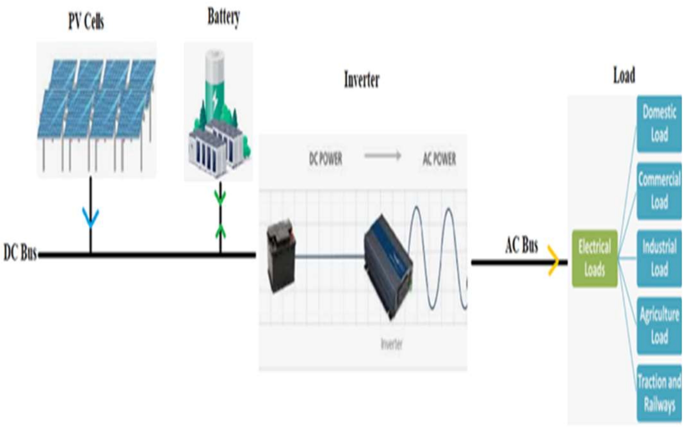

Fig. 1. Representation of PV/Load with Storage systems.

Fig. 2. Illustration of Cameroon in the World map.

Fig. 3. Illustration of Douala city in Cameroon map.

Fig. 4. Illustration of Ndogbong suburb in Douala map.

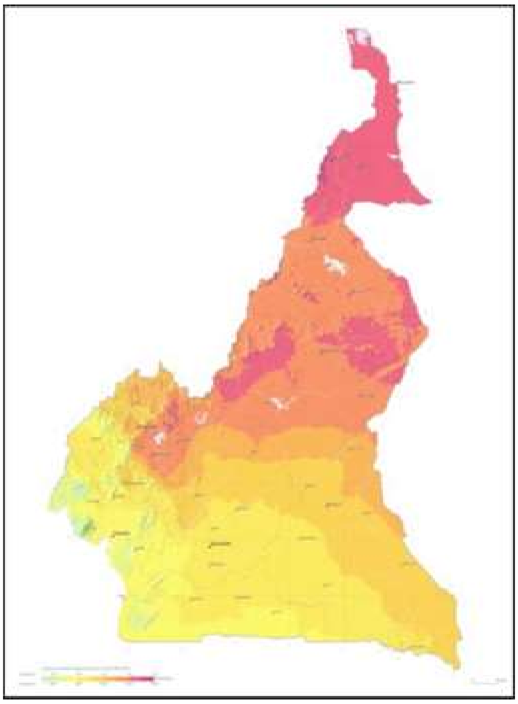

Fig. 5. Illustration of Ndogbong suburb in Douala map.

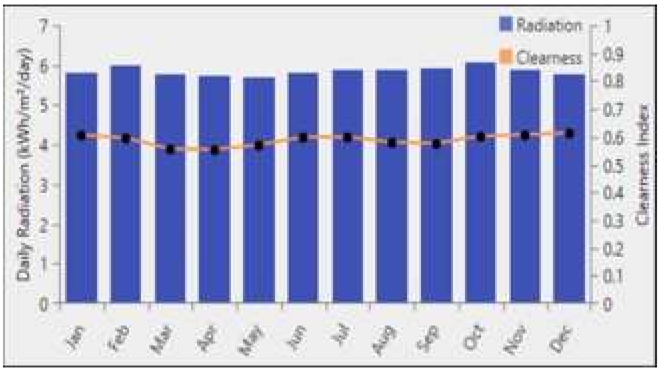

Fig. 6. Yearly representation of the solar radiation for the study area.

2.4. Hybrid renewable energy system modeling

In this work, the proposed HRES consists of PV, BSS, and DC/AC converter. In this section, a focus is put on the mathematical model of the different constituents of the HRES.

2.4.1. PV Panels

Due to the ambivalent seasons in the country, we use a mono-crystalline PV module for its advantages in warm areas [40]. The two main characteristics of the PV namely the life cycle and the efficiency have the values of 25 years and 14%, respectively. The power output of the PV is function of the solar radiation penetrating the area of the cells, the temperature, and the geolocation [41]. Authors in [42…44] proposes a formula to compute the power of the PV every hour in Eq. (1):

$$P_{PV} = f_v * P_r * \frac{G}{G_{ref}} * [1 + K_T (T_C - T_{ref})] \quad (1)$$

P_r represents the nominal power expressed in kW, G_{ref} the reference solar radiation (W/m²) whose value is 1kW/m², G is the solar radiation in W/m², f_v is the derating factor fixed at 0.9, T_{ref} is the temperature of the cell at reference conditions (∘C) with value 25∘C, K_T is the temperature coefficient with value - 4.1× 10^{-3}/∘C and Tc is calculated by the Eq. (2) [44]:

$$T_C = T_{amb} + (0.0256 * G) \quad (2)$$

T_C represents the cell temperature and T_{amb} the ambient temperature both expressed in ∘C.

(Fig. 8) presents every hour the insolation of the selected area of this study during the year 2022. All the data employed have been collected from the database of the National Aeronautics and Space Administration (NASA).

2.4.2. Inverter

In this HRES, when solar resource is not available, the inverter is in charge to convert the DC energy into AC in order to supply the load. This situation generally happens during the night and in dark hours. The efficiency of the converter is estimated at 95%. The energy conversion is essentially determined by the efficiency of the inverter but also by the type of inverter chosen. This was calculated using Eq. (3) [45].

$$\eta_{inv} = \frac{P_{inv}}{P_{in}} \quad (3)$$

Where η_{inv} and P_{in} represent respectively the efficiency and the input power of the inverter. The η_{inv} is set at 95%.

2.4.3. Battery Storage Systems

Due to the intermittency of RES, there is always a gap between demand and offer. Hence, it is important to dispose of a device in the HRES that will store the energy produced. Thus, storing excess energy will help into satisfying the system's requirements.

A battery storage system (BSS) is defined as an electrochemical device that has two roles: to store the energy at a charging state and supplies the energy stored when requested by the load at another state and under certain conditions. It is essential for HRES to cover the demand. BSS are of a great use to build up a reliable, suitable, and sustainable system. BSS plays a major role for energy management strategies. Nowadays, several technologies of BSS have been designed depending on the degree of performance, energy variations, storage abilities and other technical specifications.

When studying BSS, many criteria are to be taken into consideration. For instance, we have the ambient temperature, battery life cycle, depth of discharge (DOD), and the capacity [46]. Indeed, they have an impact on the BSS. In this paper, a 12-volt battery with a rated storage energy of 1 kWh has been employed. The permanent availability of this type of batteries which represents 70% of the whole market justifies their regular usage by scholars [47].

Many parameters like the State Of Charge (SOC) and the instantaneous power are to be considered when assessing a BSS. Those parameters depend either the BSS is on charging or discharging phase. Eqs. (4-7) model those critical parameters [48]:

a. **Charging Process:**

- Instantaneous power:

$$P_{ch}(t) = P_{PV}(t) * \eta_{ch} - \frac{P_L(t)}{\eta_{inv}} \quad (4)$$

- State Of Charge:

$$SOC(t) = (1 - \sigma) * SOC(t-1) + P_{ch}(t) \quad (5)$$

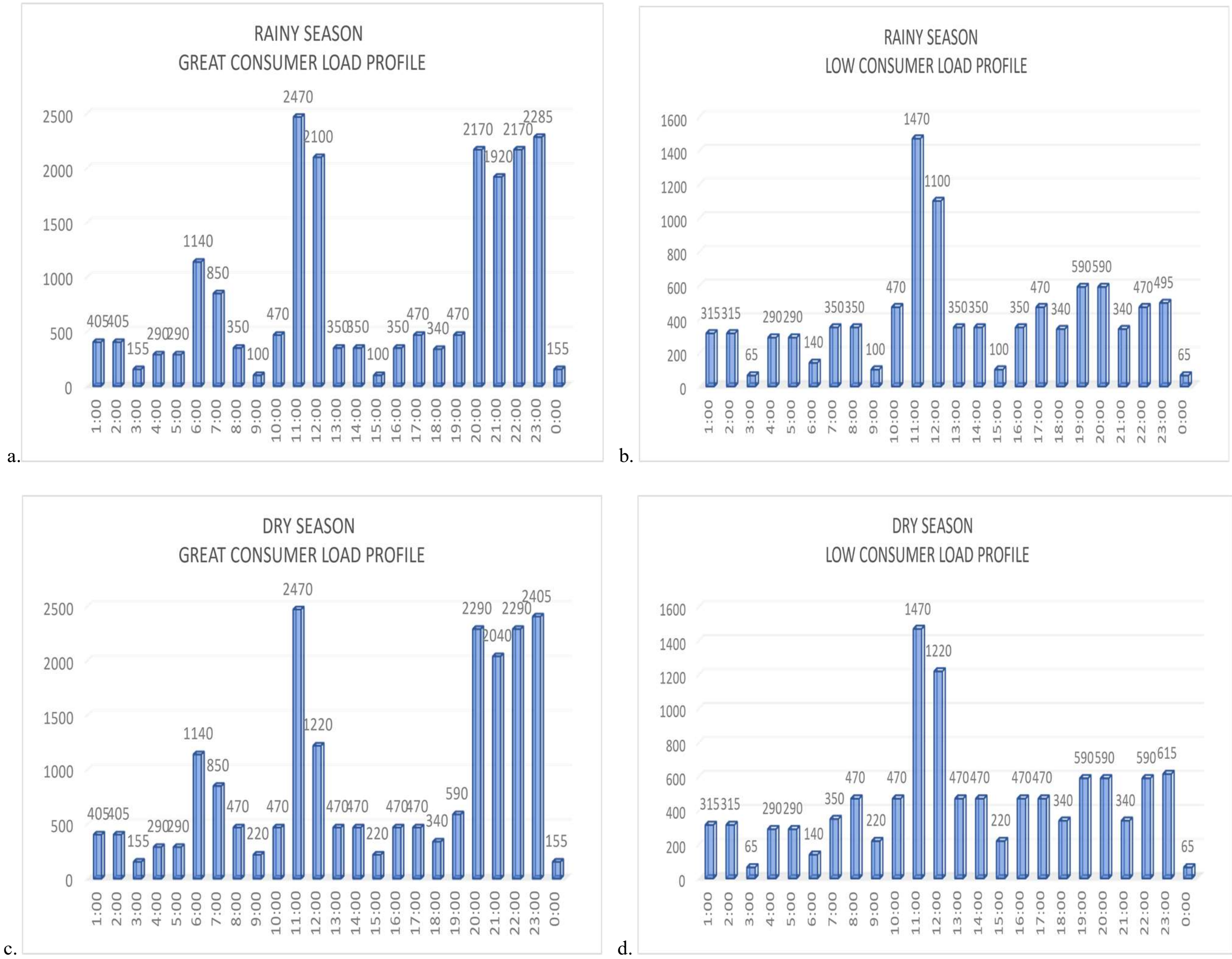

Fig. 7. Various configurations for load profile depending on rainy season for great consumer (a), low consumer (b); and dry season for great consumer (c), low consumer (d).

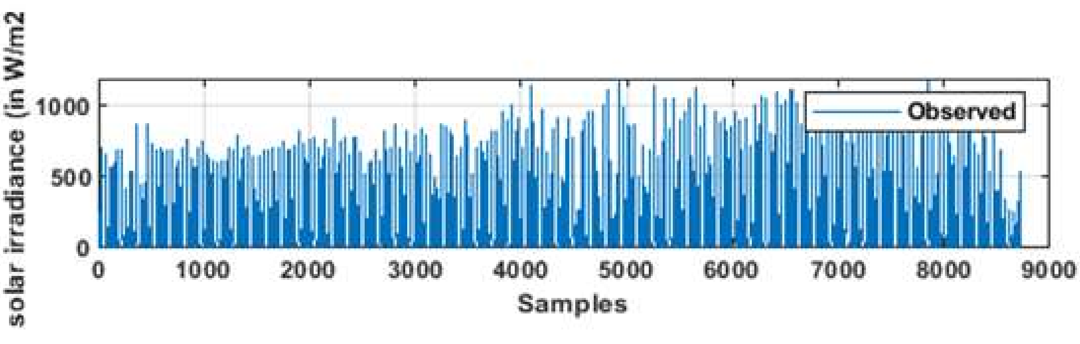

Fig. 8. Hourly radiation of the chosen site.

Table 1. Load profile for rainy season great consumer.

RAINY SEASON GREAT CONSUMER LOAD PROFILE												
EQUIPMENT	**Lamps**	**TV**	**Iron**	**Fan**	**Charger**	**Fridge**	**PC**	**Heater**	**AC**	**Micro wave**	**Washing machine**	**HOURLY ENERGY CONSUMPTION**
RATED POWER(W)	**10**	**100**	**1000**	**60**	**5**	**250**	**45**	**1000**	**1700**	**1000**	**500**	
DAILY OPERATING COMPONENTS	**100**	**18**	**2**	**8**	**25**	**16**	**10**	**2**	**4**	**1**	**1**	
DAILY ENERGY CONSUMED(Wh)	**1000**	**1800**	**2000**	**480**	**125**	**4000**	**450**	**2000**	**6800**	**1000**	**500**	
TIME (h)												
1:00	4				5	1	2					405
2:00	4				5	1	2					405
3:00	4				5		2					155
4:00	4					1						290
5:00	4					1						290
6:00	4	1								1		1140
7:00		1				1					1	850
8:00		1				1						350
9:00		1										100
10:00		1		2		1						470
11:00		1	1	2		1		1				2470
12:00		1	1					1				2100
13:00		1				1						350
14:00		1				1						350
15:00		1										100
16:00		1				1						350
17:00		1		2		1						470
18:00	12	1		2								340
19:00	12	1				1						470
20:00	12	1				1			1			2170
21:00	12	1							1			1920
22:00	12	1				1			1			2170
23:00	12	1			5	1	2		1			2285
0:00	4				5		2					155

Table 2. Load profile for rainy season low consumer.

RAINY SEASON LOW CONSUMER LOAD PROFILE							
EQUIPMENT	**Lamps**	**TV**	**Iron**	**Fan**	**Charger**	**Fridge**	**HOURLY ENERGY CONSUMPTION**
RATED POWER(W)	**10**	**100**	**1000**	**60**	**5**	**250**	
DAILY OPERATING COMPONENTS	**100**	**18**	**2**	**14**	**25**	**16**	
DAILY ENERGY CONSUMED(Wh)	**1000**	**1800**	**2000**	**840**	**125**	**4000**	
TIME(h)							
1:00	4				5	1	315
2:00	4				5	1	315
3:00	4				5		65
4:00	4					1	290
5:00	4					1	290
6:00	4	1					140
7:00		1				1	350
8:00		1				1	350
9:00		1					100
10:00		1		2		1	470
11:00		1	1	2		1	1470
12:00		1	1				1100
13:00		1				1	350
14:00		1				1	350
15:00		1					100
16:00		1				1	350
17:00		1		2		1	470
18:00	12	1		2			340
19:00	12	1		2		1	590
20:00	12	1		2		1	590
21:00	12	1		2			340
22:00	12	1				1	470
23:00	12	1			5	1	495
0:00	4				5		65

Table 3. Load profile for dry season great consumer.

DRY SEASON GREAT CONSUMER LOAD PROFILE												
EQUIPMENT	**Lamps**	**TV**	**Iron**	**Fan**	**Charger**	**Fridge**	**PC**	**Heater**	**AC**	**Micro wave**	**Washing machine**	**HOURLY ENERGY CONSUMPTION**
RATED POWER(W)	**10**	**100**	**1000**	**60**	**5**	**250**	**45**	**1000**	**1700**	**1000**	**500**	
DAILY OPERATING COMPONENTS	100	18	2	32	25	16	10	1	4	1	1	
DAILY ENERGY CONSUMED(Wh)	1000	1800	2000	1920	125	4000	450	1000	6800	1000	500	
TIME(h)												
1:00	4				5	1	2					405
2:00	4				5	1	2					405
3:00	4				5		2					155
4:00	4					1						290
5:00	4					1						290
6:00	4	1								1		1140
7:00		1				1					1	850
8:00		1		2		1						470
9:00		1		2								220
10:00		1		2		1						470
11:00		1	1	2		1		1				2470
12:00		1	1	2								1220
13:00		1		2		1						470
14:00		1		2		1						470
15:00		1		2								220
16:00		1		2		1						470
17:00		1		2		1						470
18:00	12	1		2								340
19:00	12	1		2		1						590
20:00	12	1		2		1			1			2290
21:00	12	1		2					1			2040
22:00	12	1		2		1			1			2290
23:00	12	1		2	5	1	2		1			2405
0:00	4				5		2					155

Table 4. Load profile for dry season low consumer.

RAINY SEASON LOW CONSUMER LOAD PROFILE							
EQUIPMENT	**Lamps**	**TV**	**Iron**	**Fan**	**Charger**	**Fridge**	**HOURLY ENERGY CONSUMPTION**
RATED POWER(W)	**10**	**100**	**1000**	**60**	**5**	**250**	
DAILY OPERATING COMPONENTS	100	18	2	32	25	16	
DAILY ENERGY CONSUMED(Wh)	1000	1800	2000	1920	125	4000	
TIME(h)							
1:00	4				5	1	315
2:00	4				5	1	315
3:00	4				5		65
4:00	4					1	290
5:00	4					1	290
6:00	4	1					140
7:00		1				1	350
8:00		1		2		1	470
9:00		1		2			220
10:00		1		2		1	470
11:00		1	1	2		1	1470
12:00		1	1	2			1220
13:00		1		2		1	470
14:00		1		2		1	470
15:00		1		2			220
16:00		1		2		1	470
17:00		1		2		1	470
18:00	12	1		2			340
19:00	12	1		2		1	590
20:00	12	1		2		1	590
21:00	12	1		2			340
22:00	12	1		2		1	590
23:00	12	1		2	5	1	615
0:00	4				5		65

b. **Discharging Process:**

- Instantaneous power:

$$P_{disch}(t) = \frac{P_L(t)}{\eta_{inv}} - P_{PV}(t) * \eta_{disch} \quad (6)$$

- State Of Charge:

$$SOC(t) = (1 - \sigma) * SOC(t-1) - P_{disch}(t) \quad (7)$$

In addition, the hourly power at the output of the battery is given by Eq. (8) from [49]:

$$P_{BSS} = \frac{P_L * AD}{\eta_{inv} * \eta_{bat} * DOD} \quad (8)$$

In all the relations above, $P_{ch}(t)$ and $P_{disch}(t)$ denote respectively the instantaneous power at the charging and discharging phases. η_{ch} and η_{disch} are the efficiency of the battery at the charging and the discharging phases. During discharging phase, $\eta_{disch} = 1$ and during charging phase, $\eta_{ch} = 0.8$ [50]. SOC (t) and SOC (t-1) represent the state of charge of the battery at t and (t-1) respectively. To assess the ability of the BSS to operate within the system, one critical characteristic named self-discharge denoted σ is to be considered. A value of 0.2% per day is considered for this parameter in this study [51]. Furthermore, η_{bat} represents the efficiency of the battery which is either η_{ch} during charging process or η_{disch} on discharging process. AD represents the number of autonomous days of the battery.

Many researchers establish the relations related to the constraints of a BSS to regulate its efficient operation mode. In [43, 48,52], the following Eqs. (9) and (10) have been drawn up:

$$P_{bat\,min} \leq P_{BSS} \leq P_{bat\,max} \quad (9)$$

$$DOD = 1 - \frac{P_{bat_{min}}}{P_{bat_{max}}} \quad (10)$$

$P_{bat\,min}$ and $P_{bat\,max}$ represent the respectively the lower and the upper bounds for the battery power.

The technical specifications of the study are described in Table 5.

2.5. Optimization Problem Specification

In this study, the main objective is the contribution into robust optimization by proceeding with hybridization of optimization techniques into energy management strategies to provide robust optimal solution with lowest DPSP, and best AD and Battery energy dumped. The results are obtained from comparison between separated algorithms PSO, GWO; and hybrid PSO-GWO.

The optimization part of this work will consist of both into Minimizing (Min) and Maximizing the Objective (Obj) functions given in Eqs. (11)-(13).

$$Obj1 = Min\ DPSP \quad (11)$$

$$Obj2 = Max\ AD \quad (12)$$

$$Obj3 = Max\ E_{dumped} \quad (13)$$

Subject to the following constraints:

$$0 \leq DPSP \leq 1$$

$$AD_{min} \leq AD \leq AD_{max}$$

With E_{dumped} is the energy kept into the BSS.

Table 5. Parameters of the HRES.

Parameter	Unit		Value
Inverter			
Life time Efficiency	Years %		24 92
Battery storage			
Life time Efficiency	years %		12 85
Rated power	kW		40
PV			
Life time Rated power	years kW		24 1.0
PV regulator efficiency	%		95
PV regulator cost	$/kW		150
Project life time	Years		24

2.5.1. Deficit of Power Supply Probability

DPSP is a useful parameter to assess the reliability of a system. It is calculated as the total over a year (8760h) of all the loss of power supply (DPS(t)) to the all-load power.

In a hybrid microgrid, investigating on the reliability of the system is commonly unavoidable. This is due to the sporadic behavior of the power at the output of the HRES. In this case, one parameter to take into consideration is the loss of power supply.

DPSP of a HRES can be evaluated by Eq. (14) as in [53]:

$$DPSP = \sum_{t=1}^{8760} \frac{P_L(t) - P_{RE}(t)}{P_L(t)} \quad (14)$$

Where $P_{RE}(t)$ represents the hourly power provided by the PV module and the battery storage system. Moreover, two values are possible for the DPSP namely: zero represents that all the demand is covered by the HRES and one characterizes that all the power generated by all the sources cannot satisfy at all the demand.

2.5.2. Autonomous Days

Another important parameter when it comes to assess the HRES, especially on the battery storage system, is the autonomy days. It characterizes the total duration of the battery to restore the energy stored during the charging process. A battery is assessed on this parameter as it is important and crucial. In this work, $AD_{min} = 0$ and $AD_{max} = 3$.

2.5.3. Energy Dumped into The Battery

For the system to be reliable and to have a balance demand-supply perfectly aligned, manage the energy is unaffordable. This helps into minimizing power losses and capitalizing the amount of energy saved. Henceforth, the storage systems are required in this process. Indeed, during charging phase, a certain quantity of energy is stored into battery and will be restored under certain conditions. This is a very essential part of energy management strategies.

3. Energy Management Strategy

Covering the instantly demand is crucial for reliable HRES. This implies to deploy efficient strategy and actions to fulfill this requirement. Thus, develop an efficient strategy to manage the energy within the system is required. The BSS will cover the shortage. (Fig. 9) presents a flowchart of the energy management of the hybrid renewable energy system. Firstly, the input data are at initialization step and the various conditions and constraints are established. Secondly, the energy balance is computed. The battery discharges its energy if and only if the power generated from the HRES is inferior to the load, as expressed in Eq. (15):

$$E_{disch}(t) = \left(\frac{P_L(t)}{\eta_{inv}} - P_{PV}(t) \right) * \Delta t \quad (15)$$

However, the BSS will be in charging phase when the global disposable energy provided by the HRES is greater than the demand, according to Eq. (16):

$$E_{ch}(t) = \left(P_{PV}(t) - \frac{P_L(t)}{\eta_{inv}} \right) * \Delta t \quad (16)$$

Furthermore, during the charging phase of the BSS, the excess power from solar PV is stored into the battery, expressed as follow in Eq. (17):

$$E_{dumped}(t) = P_{PV}(t) * \Delta t * \eta_{inv} - (P_L(t) * \Delta t + E_{ch}(t) * \eta_{inv}) \quad (17)$$

3.1. Objective Function

The main objective of this paper is to value the hybridization of optimization algorithms in context of robust optimization. This will result into optimal values that will simultaneously minimizing the DPSP and maximizing both the autonomous days and the energy stored into the battery. It can be illustrated in Eq. (18):

$$\min DPSP \quad (18)$$

$$\max q = \max (\lambda_1 AD + \lambda_2 E_{dumped}) \quad (19)$$

Where, λ_1,and λ_2 are parameters chosen via trial-and-error method in order to realize the optimization. At any time of the simulation, these parameters shall always globally be equal to 1.

3.2. Optimization Constraints

To achieve our main goal, some points are to be considered to allow a good computation. This constitutes the constraints of our optimization:

3.2.1. Constraints for Reliability

The technical parameter used as metric for reliability of HRES is the DPSP. Indeed, it should not exceed the acceptable value denoted β_L. Hence, the constraint related to the reliability can be written as:

$$DPSP \leq \beta_L \quad (20)$$

Furthermore, scholars proposed a value of 0.05 or 5% for β_L [53].

3.2.2. Constraints for Storage System

To ensure a better operation of the battery storage system, the SOC needs to satisfy the Eq. (21):

$$SOC_{min} \leq SOC(t) \leq SOC_{max} \quad (21)$$

Where SOC_{min} and SOC_{max} describe the interval within the state of charge of the BSS is operational.

In addition, this will ensure to have the battery always operating within its safe conditions at every time of the optimization

4. Optimization Techniques

4.1. Individual Techniques

In this paper, two methods are used to fulfill our main objective: Particle Swarm Optimization (PSO) and Grey Wolf Optimizer (GWO). These techniques are presented below:

4.1.1. Particle Swarm Optimization

Proposed by Eberhart and Kennedy (1995), PSO is a stochastic algorithm based on swarms [54]. Inspired by the nature, it is a metaheuristic technique which acts to understand the behavior of animals such as fishes, insects, birds… The efficient process to understand this technique is based on the ability of the swarms to cooperate in order to look for food.

This is mainly characterized by the path followed by swarms that learn from their previous personal activities or others. Characterized as a performant algorithm with undeniable results, it has various successful applications into some complex problems generally non-linear in nature [15].

Compared to genetic algorithms, PSO is more efficient, faster, and less complicated. Its simplicity and easy deployment into different types of problems characterize this technique as a relevant optimizer.

Three steps are to follow when implementing the PSO algorithm, namely:

- Evaluate the fitness of individual particle
- Update best finesses and positions of the local and global particles
- Update the velocity and position of individual particle

A perpetual recall of the previous best value of each particle is achieved at any step of the simulation. While iterating this process, a computation of the best fitness value among all the particles is made. This will be repeated until a defined condition is fulfilled, either a certain number of iteration is reached or a specific target fitness value is obtained. The position of each particle in the swarm is updated using the following equation:

$$x_{k+1}^{i} = x_{k}^{i} + v_{k+1}^{i} \quad (22)$$

Where x_k^i and v_k^i are respectively i-particle position and velocity in iteration k. The velocity is calculated as followed:

$$v_{k+1}^{i} = k \times [v_k^i + c_1 r_1 (p_k^i - x_k^i) + c_2 r_2 (p_k^g - x_k^i) \quad (23)$$

$$k = \frac{2}{2 - \emptyset - \sqrt{\emptyset^2 - 4\emptyset}} \quad (24)$$

$$\emptyset = c_1 - c_2;\ \emptyset > 4 \quad (25)$$

- p^i represents the best particle position for an individual while p^g is the best global position; the social and cognitive parameters are denoted c_1 and c_2; whereas r_1 and r_2 are two real values within internal 0 and 1.
- v_k^i, called inertia, determines the fact that particles have the following identical characteristics: same direction and same velocity.
- $c_1 r_1 (p_k^i - x_k^i)$, is the cognitive component, causing the particle return to a previous position in which it has experienced high individual fitness.
- $c_2 r_2 (p_k^g - x_k^i)$, represents the social component, which makes the particle to adhere to the best region identified by the swarm and to follow the best direction all around. Two considerations can be done concerning c_1 and c_2 : when $c_1 >> c_2$, hence each particle will follow the individual best position; but when $c_2 >> c_1$, then particles will move to the global best position. In this study the value of certain parameters is optimized by using PSO.

The flowchart of the PSO is presented in (Fig. 10).

4.1.2. Grey Wolf Optimizer

Proposed by Mirjalili in 2014 [50], this technique is based on the attitude of wolves while hunting. To capture the prey, wolves implement a good organization which ranked them on top of predators. They are adequate for the social life, and to preserve their collaborative identity of hunters, a rough social hierarchy is established among them. While modeling the social hierarchy and hunting process of the wolves, three phases are required, (Fig.11): search (a), encircle (b), and attack the prey (c,d,e). This has highly inspired GWO [50].

4.1.2.1. Social Hierarchy

Four parameters allow to classify grey wolves, especially (α, β, δ and ω). While it comes to decide on the hunting, the leader called (α) is the best answer to this call. (Fig. 12) clearly illustrates this statement. The next level while hunting the prey named (β) is of a great help to the alpha when attacking the prey. The following step called delta (δ) and the rest of the grey wolves assumed to be omega (ω), constitute the subsets that follow the three wolves α, β, and δ.

4.1.2.2. Encircling Prey

Eqs. (26) and (27) present the optimal updates values of the positions of the wolves:

$$|\vec{W} = Q * \vec{Y}_p(t) - Y(t)| \quad (26)$$

$$\vec{D}(t+1) = \vec{Y}_p(t) - C(\vec{W}) \quad (27)$$

Where t represents the current iteration, the coefficient vectors are denoted $\vec{C}$ and $\vec{Q}$, x_p is the vector that represents the position of the prey, and $\vec{D}$ is a vector that represents the position of the wolf. Eqs. (28 and 29) compute the vectors $\vec{C}$ and $\vec{Q}$:

$$\vec{C} = 2 * \vec{r} * \vec{a_1} - \vec{r} \quad (28)$$

$$\vec{Q} = 2 * \vec{a_2} \quad (29)$$

Where $\vec{r}$ is the vector of components that varies within 0 and 2 over all iterations. a_1 and a_2 are two random real numbers chosen in the interval [0, 1].

4.1.2.3. Behavior of Hunting

Firstly, after determining the location of the prey, the grey wolves encircle it to hunt. Then, the three leaders (α), (β), and (δ) will decide and collaborate in the hunting process. Hence, the three best solutions are defined α, β, and δ, while the other search agents (as well as omegas) will contribute into updating the positions corresponding to the status of the best agent.

The mathematical model for grey wolf hunting is shown in Eqs. (30 - 32):

$$|\vec{W_\alpha} = Q_1 * Y_\alpha - Y| \quad (30)$$

$$|\vec{W_\beta} = Q_2 * Y_\beta - Y| \quad (31)$$

$$|\vec{W_\delta} = Q_3 * Y_\delta - Y| \quad (32)$$

Where Y_α, Y_β, and Y_δ are the first three best solutions in each iteration. The actual position of a search agent (omega wolves) from each best solution is given by Eqs. (33 - 35):

$$\vec{Y}_1 = \vec{Y}_\alpha - A_1 * (\vec{W_\alpha}) \quad (33)$$

$$\vec{Y}_2 = \vec{Y}_\beta - A_2 * (\vec{W_\beta}) \quad (34)$$

$$\vec{Y}_3 = \vec{Y}_\delta - A_3 * (\vec{W_\delta}) \quad (35)$$

$$\vec{Y}(t+1) = \frac{\vec{Y}_1 + \vec{Y}_2 + \vec{Y}_3}{3} \quad (36)$$

(Fig. 13) depicts Eq. (36), showing the process to update the position of a search agent randomly, allowing α, β, and δ in the search space area [50]. The various positions of the wolves around the prey are updated. (Fig. 14) describes the flowchart of the GWO.

4.2. Hybrid Technique: Particle Swarm Optimization – Grey Wolf Optimizer:

In context of robust optimization, a hybridization is performed between PSO and GWO for more efficient optimization algorithm. In addition, many parameters are to be optimized. Henceforth, we are performing Multi-Objective Optimization (MOO). This was proposed by COELLO [55], especially for PSO (MOPSO). Furthermore, in MOPSO, all particles shared all the information. This will help them moving towards the global best particles and their own best memory. A temporary external back up memory is used to keep non-dominated solutions of the population at the end of each iteration.

In comparison of the PSO, GWO offers two advantages: a high probability to avoid the local optima and a perfect ability of exploration. In GWO, the initialization is not required. Indeed, this is due to the fact that the initial set of population of PSO constitutes the primary sorted population of GWO. Although GWO is a Single-Objective Optimization (SOO), it produces child population G of the same size as the parent population. This implies to have the positions given by the GWO updated and sorted according to the fitness value obtained at each iteration. The algorithm stops processing while it reaches the upper limit of iterations; otherwise, it continues, as depicted in (Fig. 15). Therefore, the hybrid algorithm combines the resourcefulness of both techniques to provide by the end a much more reliable delivery.

5. Results and Discussions

Two optimization algorithms are used in this paper to obtain optimal results. The meteorological data of four types of houses in the area located combined with the technical parameters were imposed on the simulations executed through the algorithms of PSO, GWO and hybrid PSO-GWO. The constituents of the chosen HRES used are PV and BSS in a stand-alone configuration. Optimization algorithms were performed on the designed HRES for 100 maximum numbers of iterations and 10 particles for population. Results were generated with MOO algorithms coded in MATLAB R2018a environment. The input parameters of the problem are given in Table 6. The different meteorological data comprising the solar radiation and the temperature on hour basis all over a complete year (8760 h) and each specific type of load were used in this study.

Furthermore, four houses have been considered according to the number of apparatuses. This has been segregated as follows:

- Load 1: rainy season low consumer
- Load 2: rainy season great consumer
- Load 3: dry season low consumer
- Load 4: dry season great consumer

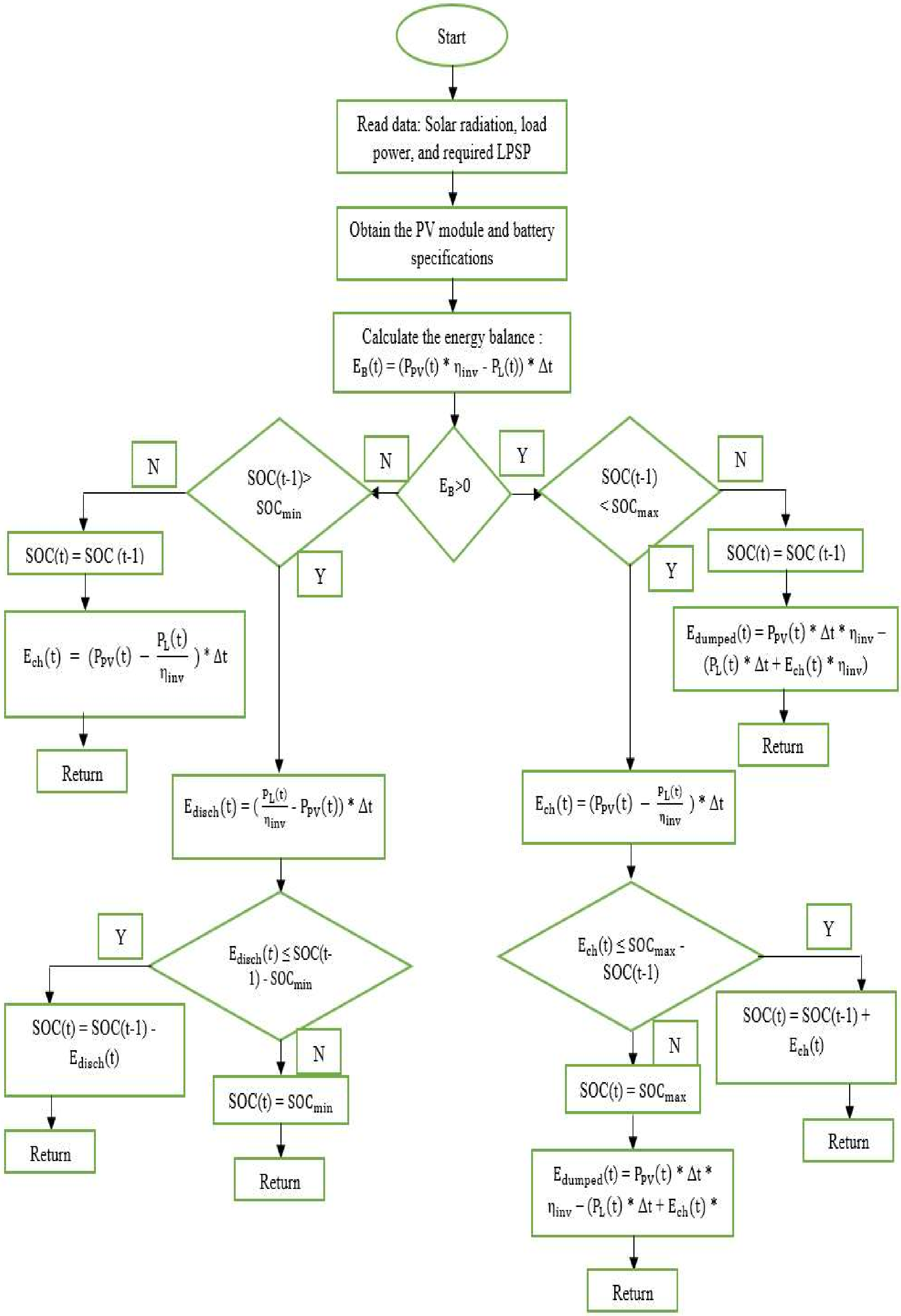

Fig. 9. Flow chart of the operation mode of the HRES.

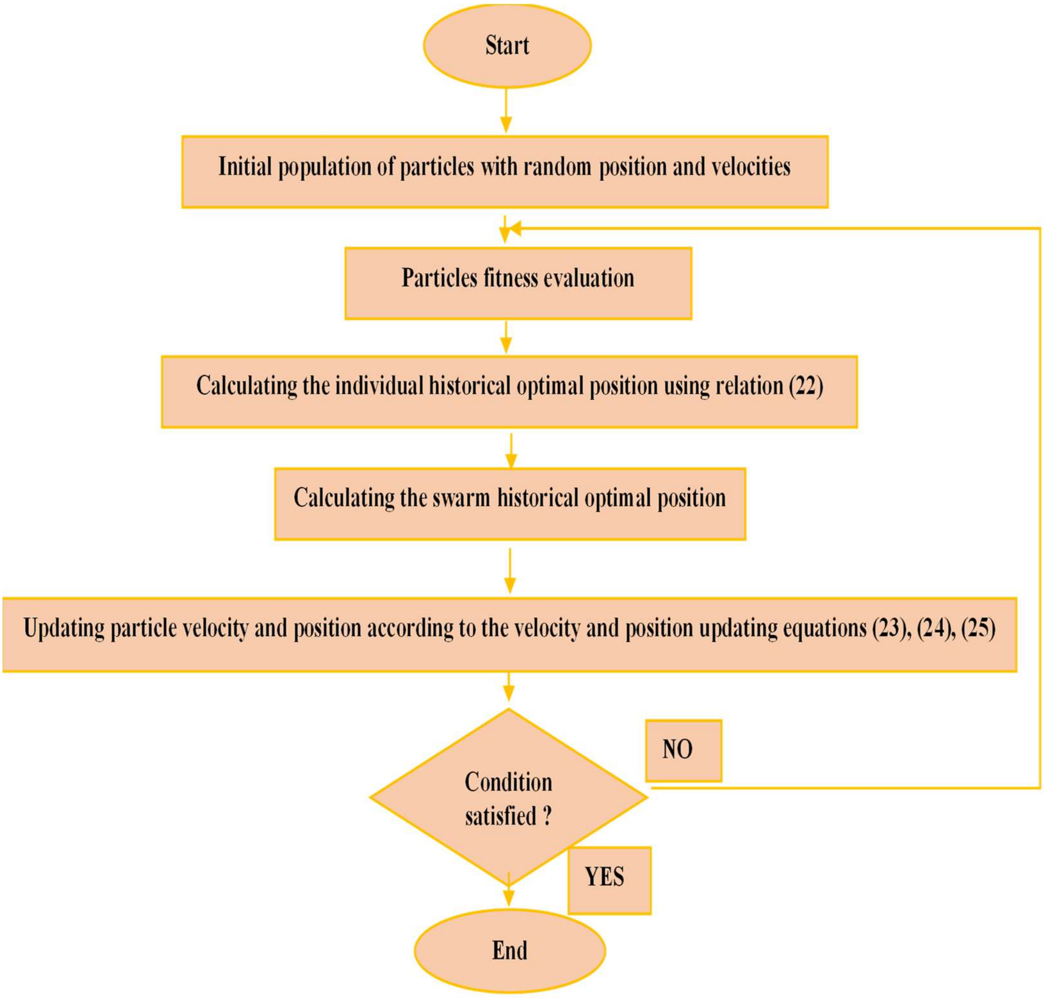

Fig. 10. Flowchart of the particle swarm optimization algorithm.

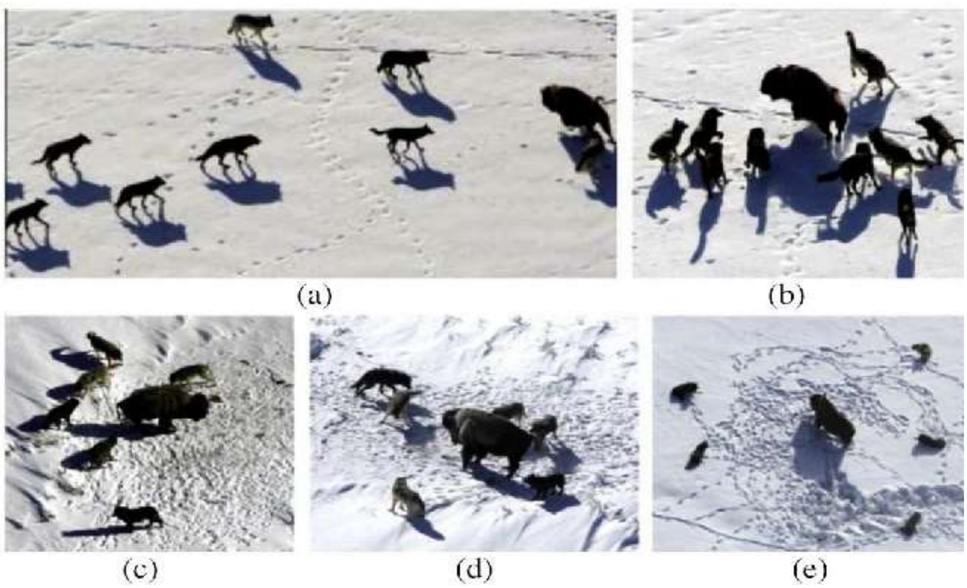

Fig. 11. Haunting process of Grey Wolves.

Fig. 12. Social hierarchy of Grey Wolves.

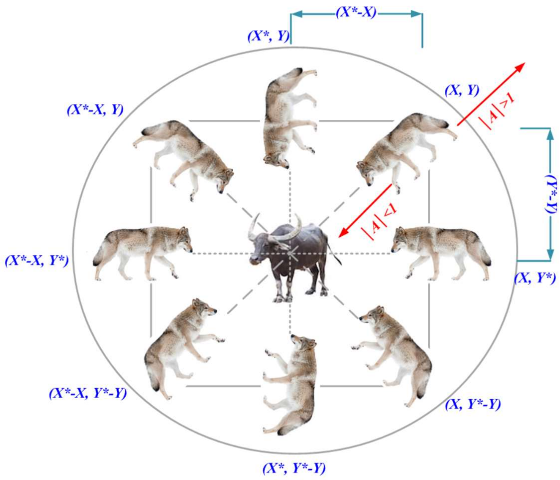

Fig. 13. Position updating mechanism of search agents.

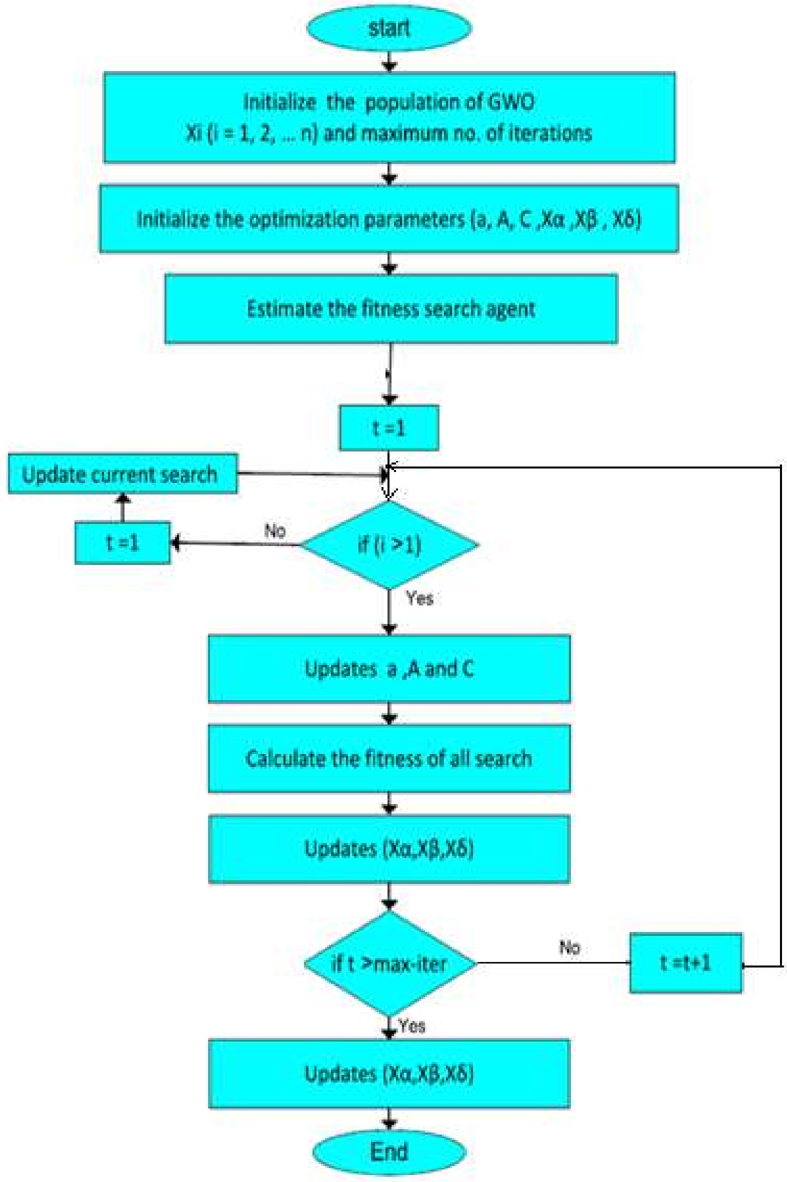

Fig. 14. Flowchart of the Grey Wolf Optimizer.

The results presented in Table 7 clearly illustrate that best results are obtained with hybrid algorithm. With the energy conservation demand side management (DSM) strategy implemented, the optimization of the hybrid energy is performed on the four various loads with the three algorithms. Indeed, for all the loads, the system is more reliable with better autonomy while performing PSO-GWO algorithm. This is visible for instance for load 1 with a DPSP of 4.21%, a good autonomy (2.5 days) and the amount of energy stored into the battery is higher (2.77kW). In comparison, the two techniques individually offer great results for DPSP accepted as stated in [53], but not as good as the hybrid PSO-GWO. In addition, as shown in (Fig. 7), the great consumer in dry season (load 3) represents the biggest one among the 4 types. The results obtained after performing the simulation for load 3 are still the same, showing that hybridization constitutes a good step into robust optimization. (Figs. 16-19) depicts the simulation results for all loads.

Table 7. Results of the simulations.

	LOAD 1		
Parameters Optimization	**DPSP(%)**	**AD**	**Edumped(kW)**
PSO	4.71	1.8	2.51
GWO	4.91	1.9	2.61
PSO-GWO	4.21	2.5	2.77
	LOAD 2		
Parameters Optimization	**DPSP(%)**	**AD**	**Edumped(kW)**
PSO	1.47	2.1	6.124
GWO	1.405	2.5	6.413
PSO-GWO	1.375	3	6.742
	LOAD 3		
Parameters Optimization	**DPSP(%)**	**AD**	**Edumped(kW)**
PSO	3.61	1.5	2.87
GWO	3.72	1.4	2.67
PSO-GWO	1.04	2.2	2.95
	LOAD 4		
Parameters Optimization	**DPSP(%)**	**AD**	**Edumped(kW)**
PSO	1.21	2.1	6.824
GWO	1.36	2.4	6.613
PSO-GWO	1.01	2.9	7.013

6. Statistical Analysis

Table 6. Parameters of the optimization algorithms.

Parameters of PSO	
chi1	**0.81**
chi2	**0.81**
Parameters of GWO	
r1	**0.5**
r2	**0.5**
a	**2**

Those parameters can be presented by the above relations:

$$SD = \sqrt{\frac{\sum_{i=1}^{n_{sim}}(Y_i - \bar{Y})}{n_{sim}}} \quad (37)$$

$$RMSE = \sqrt{\frac{\sum_{i=1}^{n_{sim}}(Y_i - Y_{min})^2}{n_{sim}}} \quad (38)$$

$$RE = \frac{\sum_{i=1}^{n_{sim}}(Y_i - Y_{min})}{Y_{min}} \quad (39)$$

$$MAE = \frac{\sum_{i=1}^{n_{sim}}(Y_i - Y_{min})}{Y_{min}} \quad (40)$$

$$Efficiency = \frac{Y_{min}}{Y_i} \quad (41)$$

Where Y_i corresponds to the DPSP for the chosen technique at each simulation. While Y_{min} represents the best value obtained, and n_{sim} is the total simulations achieved with MATLAB software. In this work, the following parameters have been employed to obtain optimal and efficient results: search agents = 10, iterations number in each simulation = 100, and executions number of simulations for each method = 35 simulations.

Table 8 describes the statistical performance of PSO, GWO and PSO-GWO. In this table, the value of SD obtained demonstrates the stability of the PSO-GWO compared with the two other techniques throughout the simulations and has an acceptable RMSE. The results indicate that the PSO and PSO-GWO have close values in the majority of the 35 simulations, while the GWO optimization technique arrives hard fully at the optimum solution. Alike, the optimization algorithms efficiency is 99.62%, 98.11%, and 99.87% for PSO, GWO, and PSO-GWO respectively. In addition, the average best value in the 30 runs shows the PSO-GWO results can be suggested as the better optimal solution of the objective function, has the small deviations, and has the superiority in solving the optimization problem, followed by PSO, and

GWO, correspondingly. (Fig. 20) presents the efficiency of the three methods employed in this study.

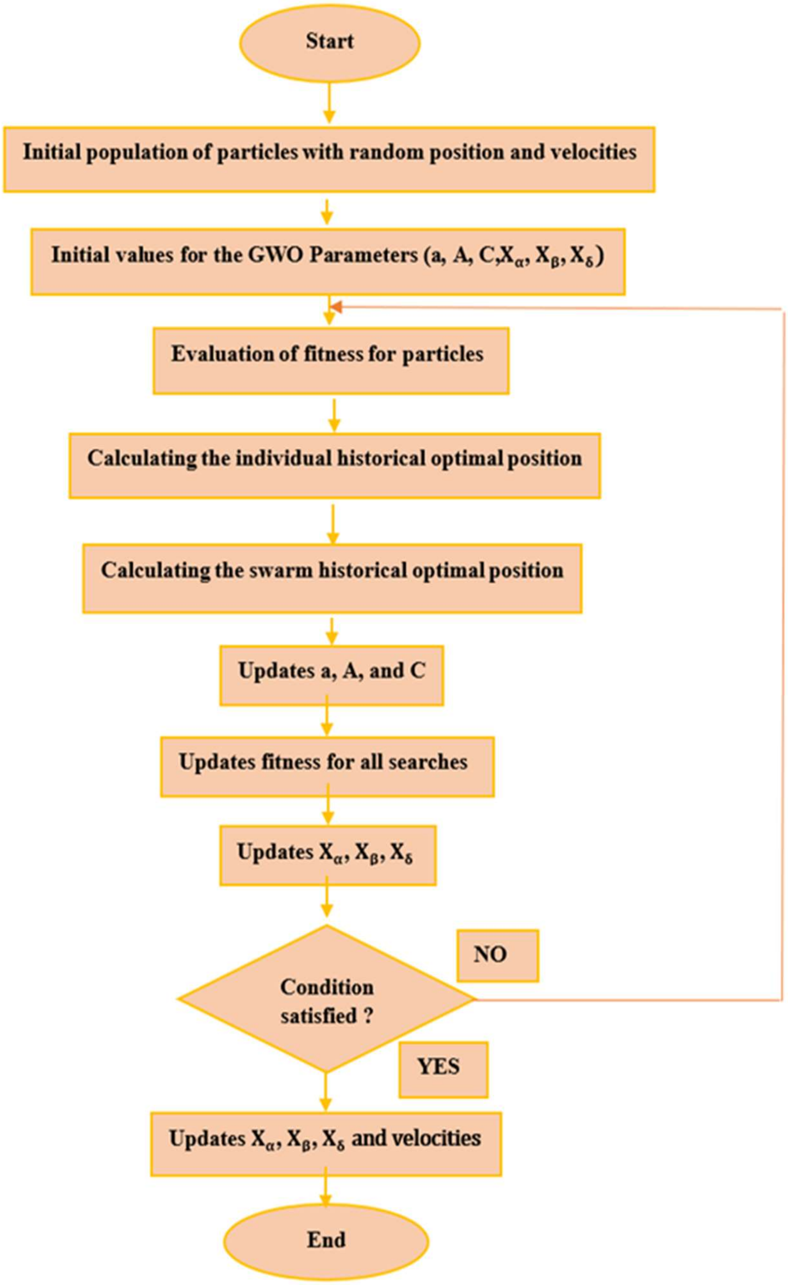

Fig. 15. Flowchart of the Particle Swarm Optimization - Grey Wolves Optimizer.

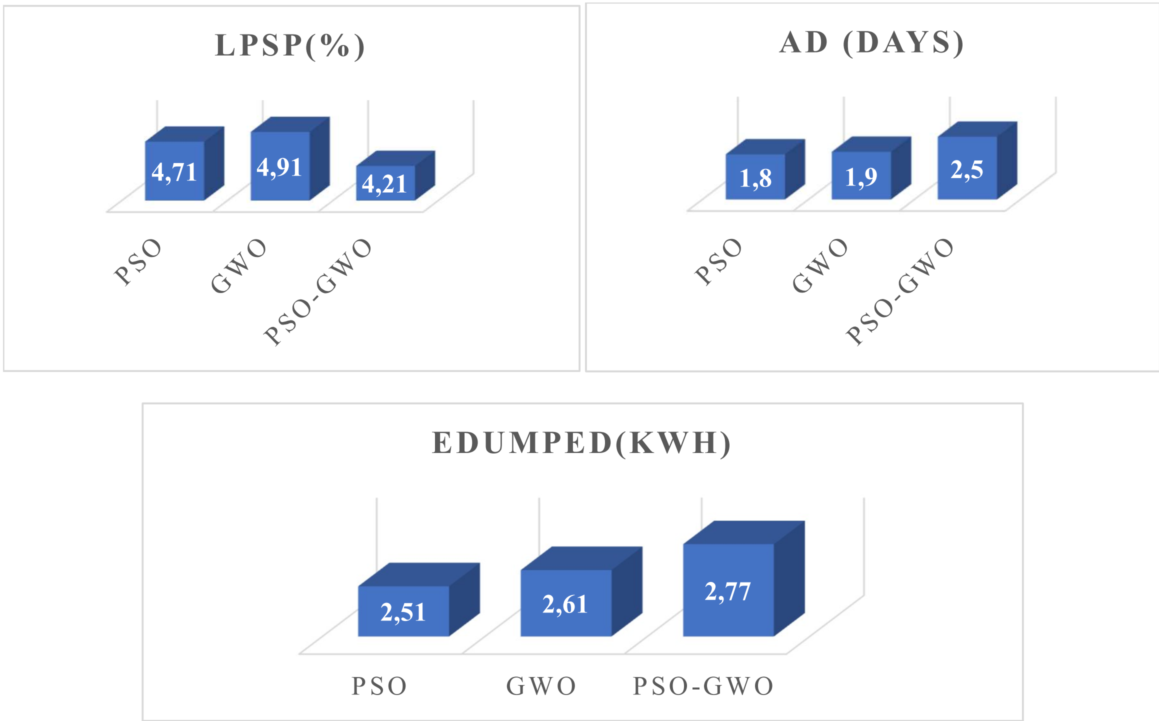

Fig. 16. Results of the simulation for load 1.

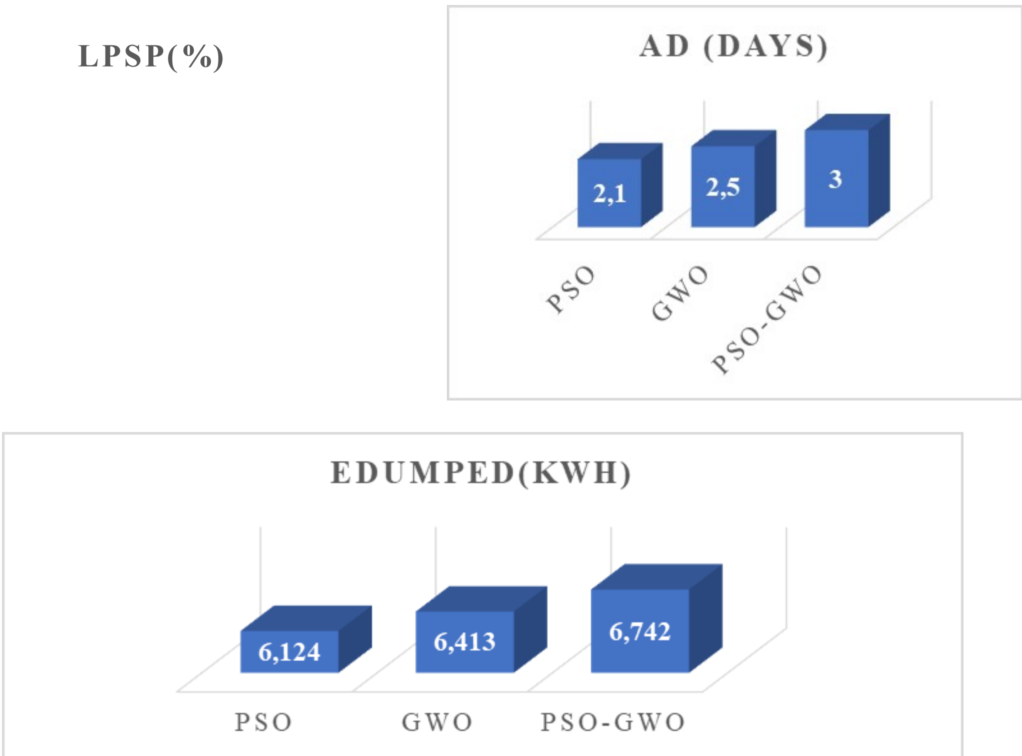

Fig. 17. Results of the simulation for load 2.

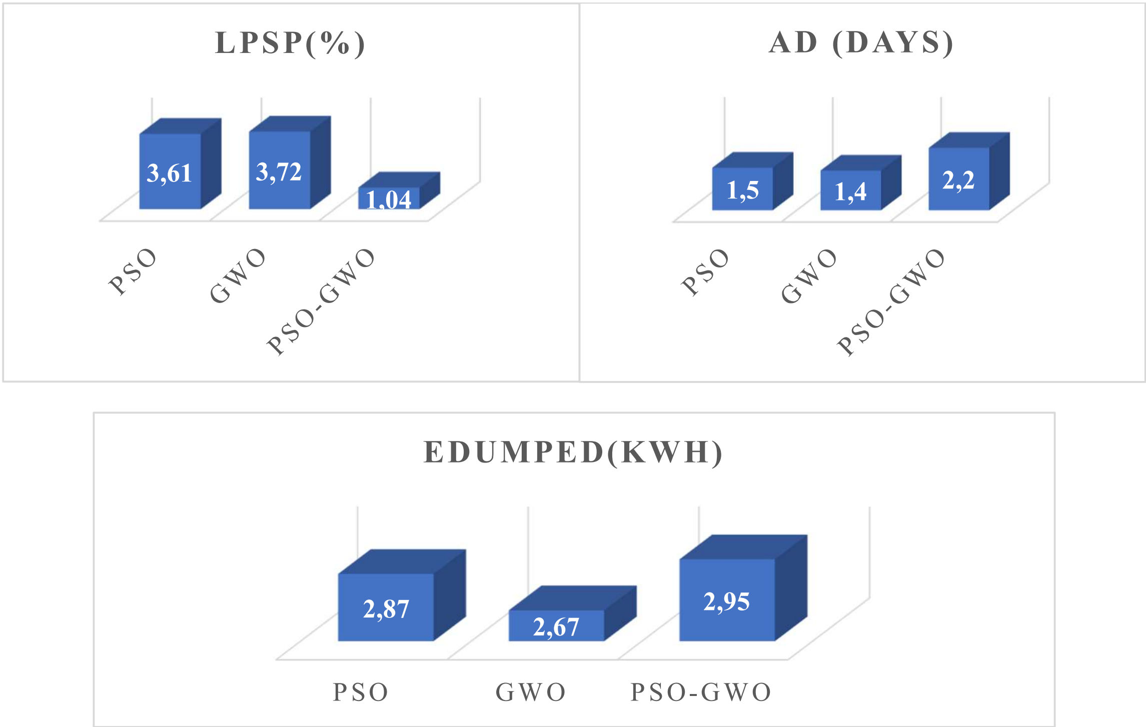

Fig. 18. Results of the simulation for load 3.

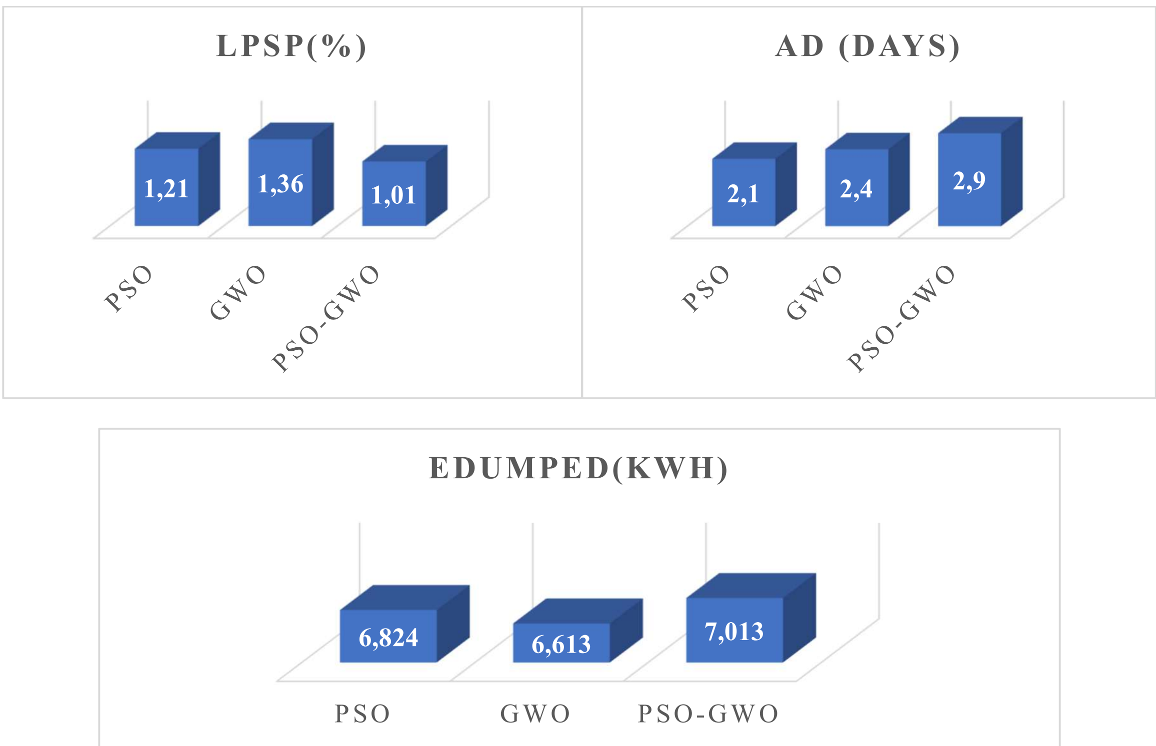

Fig. 19. Results of the simulation for load 4.

Table 8. Statistical results of PSO, GWO and PSO-GWO techniques.

Optima. Technique	Max.	Min.	Average	Median	SD	Average RE	MAE	RMSE	Efficiency
PSO	4.72	1.21	2.965	2.971	0.11	0.656	0.0023	0.0037625	99.62%
GWO	4.93	1.36	3.145	3.148	0.15	0.0094	0.00005	0.00007976	98.11%
PSO-GWO	4.23	1.01	2.62	2.65	0.07	0.0112	0.00004	0.00007966	99.87%

7. Conclusion

In this paper, a methodology of an optimal solution of a stand-alone HRES comprising PV, BSS via three metaheuristic techniques is described. Four types of loads have been selected in a located area in Douala Cameroon according to their life conditions. PSO, GWO and PSO-GWO have been employed in this study to assess and improve the reliability and the autonomy of the HRES. Simulations have been performed with MATLAB R2018a environment. In this study, two nature-inspired algorithms PSO and GWO were hybridized to proceed to the optimization, focusing on DPSP, autonomous days and energy stored into the battery as decision variables. The main objective was to find the minimum DPSP and maximum autonomy by varying types of loads and providing all the optimal solutions. At the end of the study, the developed hybrid algorithm has a high probability while achieving the global optimum solution. A much better efficiency, a lower DPSP, a lower mean are also some advantages offered by hybridization. Henceforth, hybridization of HRES is more accurate while being under uncertainty conditions (load, meteorological data). From the lowest to the highest consumer, PSO-GWO provides better reliability and autonomy.

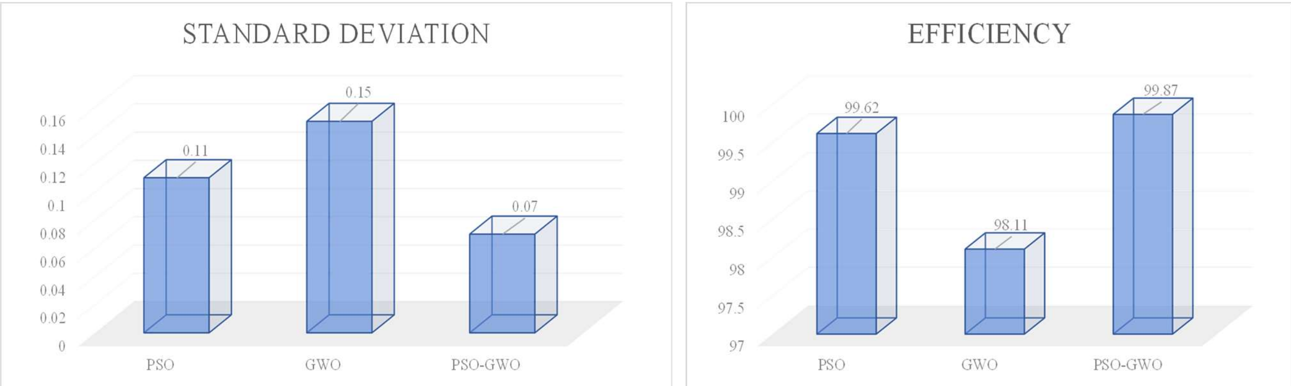

Fig. 20. Statistical results comparison between of PSO, GWO, and PSO-GWO.

Acknowledgements

No acknowledgments.

References

[1] N. Norouzi. The Pahlev Reliability Index: A measurement for the resilience of power generation technologies versus climate change. Nucl. Eng. Technol. **2021**, 53, 1658–1663.

[2] S.H. Nengroo; H. Jin; S. Lee. Management of Distributed Renewable Energy Resources with the Help of a Wireless Sensor Network. *Appl. Sci.* **2022**, *12*, 6908.

[3] J.K. Kaldellis, D. Zafirakis, 2011. The wind energy (r) evolution: A short review of a long history. Renew. Energy 36 (7), 1887–1901.

[4] V. Khare, S. Nema, Baredar, Prashant, 2016. Solar–wind hybrid renewable energy system: A review. Renew. Sustain. Energy Rev. 58, 23–33.

[5] Y. Sawle; S.C. Gupta; A.K. Bohre. Review of Hybrid Renewable Energy Systems with Comparative Analysis of Off-Grid Hybrid System. *Renew. Sustain. Energy Rev.* **2018**, *81*, 2217–2235.

[6] IEA,IndiaEnergy Outlook. Paris, 2015, http://www.iea.org/publications/freepublications/publication/africa-energy-outlook.html. Consulted on January 2023.

[7] N. Ouedraogo. Modeling sustainable long-term electricity supply–demand in Africa. Appl. Energy 2017; 190:1047–67. http://dx.doi.org/10.1016/j.apenergy.2016.12.162.

[8] M.Z. Jacobson; Delucchi, M.A. Providing All Global Energy with Wind, Water, and Solar Power, Part I: Technologies, Energy Resources, Quantities and Areas of Infrastructure, and Materials. *Energy Policy* **2011**, *39*, 1154–1169.

[9] F.M. Wulfran, S. R. DZONDE NAOUSSI, R. J. J. MOLU, S.T. Kenfack, Demand-Supply Forecasting based on Deep Learning for Electricity Balance in Cameroon, EconJournals. IIJEEP 2022, 12(4), 99-103;

[10] S. Guefano, J.G. Tamba, E.W. Azong, L. Monkam, (2020), Forecast of electricity consumption in the residential sector by Grey and autoregressive models. Energy, 214, 1-14 (2020).

[11] S.S. Qarnain; S. Muthuvel; S. Bathrinath. Review on government action plans to reduce energy consumption in buildings amid COVID-19 pandemic outbreak. Mater. Today Proc. **2021**, 45, 1264–1268.

[12] S. K. Debrah, M. A. Nyasapoh, F. Ameyaw, S. Yamoah, N. K. Allotey, and F. Agyeman, "Drivers for nuclear energy inclusion in Ghana's energy mix," Journal of Energy, vol. 2020, Article ID 8873058, 12 pages, 2020.

[13] A. Srivastav, "Energy Security and Sustainability: An Overview," in Advances in Geographical and Environmental Sciences, pp. 1–31, Springer, Singapore, 2021.

[14] D.N. Karamov; P.V. Ilyushin; K.V. Suslov. Electrification of Rural Remote Areas Using Renewable Energy Sources: Literature Review. Energies 2022, 15, 5881. https://doi.org/10.3390/ en15165881

[15] N. Alshammari, J. Asumadu, 2020. Optimum unit sizing of hybrid renewable energy system utilizing harmony search, Jaya and particle swarm optimization algorithms. Sustain. Cities Soc. 60, 102255.

[16] M. K. Amaehule, R. Uhunlwangho, N. Nwazor, E. S. Mbonu, K. E. Okedu. Investigation of the Impact of Soot on the Efficiency of Solar Panels using a Smart Intelligent Monitoring System. International Journal of Smart Grid, Vol.7, No. 1, March, 2023.

[17] K.E. Sarah, K.E. Okedu, R. Uhunmwagho. Harnessing Solar and Wind Power for Hybrid Stand-alone Energy System : The Case of Coastline Communities in Delta State of Southern Nigeria. International Journal of Smart Grid, Vol.7, No. 1, March, 2023.

[18] S.H. Nengroo; M.U. Ali; A. Zafar; S. Hussain; T. Murtaza; M.J. Alvi; K. Raghavendra; H.J. Kim. An Optimized Methodology for a Hybrid Photo-Voltaic and Energy Storage System Connected to a Low-Voltage Grid. *Electronics* **2019**, *8*, 176.

[19] S.H. Nengroo; S. Lee; H. Jin; D. Har. Optimal Scheduling of Energy Storage for Power System with Capability of Sensing Short-Term Future PV Power Production. In Proceedings of the 11th International Conference on Power and Energy Systems (ICPES), Shanghai, China, 18–20 December 2021 ; IEEE : Piscataway, NJ, USA, 2021 ; pp. 172–177.

[20] A. Maleki; F. Pourfayaz. Optimal Sizing of Autonomous Hybrid Photovoltaic/Wind/Battery Power System with DPSP Technology by Using Evolutionary Algorithms. *Sol. Energy* **2015**, *115*, 471–483.

[21] A.A. Khan ; A.F. Minai ; R.K. Pachauri ; H. Malik. Optimal Sizing, Control, and Management Strategies for Hybrid Renewable Energy Systems: A Comprehensive Review. *Energies* **2022**, *15*, 6249. https://doi.org/10.3390/en15176249.

[22] T. Chowdhury ; S. Hasan ; H. Chowdhury ; A. Hasnat; A. Rashedi; M.R.M. Asyraf.; M.Z. Hassan; S.M. Sait. Sizing of an Island Standalone Hybrid System Considering Economic and Environmental Parameters: A Case Study. *Energies* **2022**, *15*, 5940. https://doi.org/10.3390/en15165940.

[23] A. Mahesh, K.S. Sandhu, 2020. A genetic algorithm based improved optimal sizing strategy for solar-wind-battery hybrid system using energy filter algorithm'' front. Energy 14 (1), 139–151.

[24] G. Lei; H. Song; D. Rodriguez. Power generation cost minimization of the grid-connected hybrid renewable energy system through optimal sizing using the modified seagull optimization technique. Energy Rep. 2020, 6, 3365–3376.

[25] M.A.E.S. Badr. Hybrid Wind and Solar Systems Optimization. In Modeling, Simulation and Optimization of Wind Farms and Hybrid Systems ; IntechOpen : London, UK, 2020 ; p. 262.

[26] T.H. Djeudjo, Njomo Donatien, F.A. Talla Konchou, Tchinda René, Techno-economic and environmental feasibility study with demand-side management of photovoltaic/wind/hydroelectricity/battery/diesel : A case study in Sub-Saharan Africa. Energy Conversion and Management 258 (2022) 115494

[27] A.S. A.-Buraiki, A. A.-Sharafi. 2021. Technoeconomic analysis and optimization of hybrid solar/wind/battery systems for a standalone house integrated with electric vehicle in Saudi Arabia. Energy Convers. Manage. 250 (14899).

[28] D. Das ; R. Esmaili, L. Xu ; D. Nichols. An optimal design of a grid connected hybrid wind/photovoltaic/fuel cell system for distributed energy production. In Proceedings of the 31st Annual Conference of IEEE Industrial Electronics Society, IECON 2005, Raleigh, NC, USA, 6–10 November 2005 ; p. 6.

[29] N. Ghorbani, A. Kasaeian, A. Toopshekan, L. Bahrami, A. Maghami, 2017. Optimizing a hybrid wind-PV-battery system using GA-PSO and MOPSO for reducing cost and increasing reliability. Energy http://dx.doi.org/10.1016/j.energy.2017.12.057.

[30] J.A. Nieves ; A.J. Aristizábal; I. Dyner; O. Báez; D.H. Ospina. Energy demand and greenhouse gas emissions analysis in Colombia: A LEAP model application. Energy **2019**, 169, 380–397.

[31] C. Li ; X. Ge ; Y. Zheng ; C. Xu ; Y. Ren ; C. Song ; C. Yang. Techno-Economic Feasibility Study of Autonomous Hybrid Wind/PV/Battery Power System for a Household in Urumqi, China. *Energy* **2013**, *55*, 263–272.

[32] M.R. Islam ; H. Akter ; H.O.R Howlader ; T. Senjyu. Optimal Sizing and Techno-Economic Analysis of Grid-Independent Hybrid Energy System for Sustained Rural Electrification in Developing Countries : A Case Study in Bangladesh. *Energies* **2022**, *15*, 6381. https://doi.org/10.3390/en15176381.

[33] R.J.J. MOLU, W.F. Mbasso, S.R.D. NAOUSSI, S.T. Kenfack, P. Wira, Investigating the dependency between electricity and the human development based on metaheuristic optimization, EconJournals. IIJEEP 2022, 12, 55-60;

[34] R.H.T. Djiela, P.T. Kapen, G. Tchuen. Techno-economic design and performance evaluation of Photovoltaic/

Diesel/Batteries system through simulation of the energy flow using generated solar radiation data. Energy Convers Manage 2021 ; 248 :114772.

[35] The World Bank, "Access to electricity (% of population) - Sub-Saharan Africa : Data," 2022. Consulted on January 2023.

[36] S. Fayza, A.M. Mahmoud. A. A. Abdelhamid, A.-H. M. Sumaiti, A.A. El-Sayed, Zaki Diab. Sizing and design of a pv-wind-fuel cell storage system integrated into a grid considering the uncertainty of load demand using the marine predators algorithm. Mathematics 2022, 10, 3708.

[37] "World Weather Information Service – Douala". World Meteorological Organization. Retrieved 13 June 2016. Consulted on January 2023

[38] S. Rajanna, R.P. Saini. Employing demand side management for selection of suitable scenario-wise isolated integrated renewal energy models in an Indian remote rural area. Renewable Energy 2016 ; 99 :1161–80.

[39] D. Shi ; R. Li ; R. Shi ; F. Li. Analysis of the relationship between load profile and weather condition. In Proceedings of the 2014 IEEE PES General Meeting Conference & Exposition, National Harbor, MD, USA, 27–31 July 2014 ; pp. 1–5.

[40] N.S. Baghel ; N. Chander. Performance comparison of mono and polycrystalline silicon solar photovoltaic modules under tropical wet and dry climatic conditions in east-central India. Clean Energy 2022, 6, 165–177.

[41] H. Yang ; Z. Wei ; L. Chengzhi. Optimal design and techno-economic analysis of a hybrid solar–wind power generation system. Appl. Energy 2009, 86, 163–169.

[42] M.A. Elhadidy, 2002. Performance evaluation of hybrid (wind/solar/diesel) power systems. Renew. Energy 26 (3), 401–413.

[43] K.M. Kotb, M.R. Elkadeema, M.F. Elmorshedy, A. Dan. Coordinated power management and optimized techno-enviro-economic design of an autonomous hybrid renewable microgrid: A case study in Egypt. Energy Convers Manag 2020 ;221(113185). https://doi.org/10.1016/j.enconman.2020.113185.

[44] D.T. Hermann, N. Donatien, T.K.F. Armel, T. René. A Feasibility Study Of An On-Grid PV/Wind/Battery/Diesel For Residential Buildings Under Various Climates In Cameroon. Energy Technology 2021 ;9(12) :2100615.

[45] M.U.R. Tahir ; A. Amin ; A.A. Baig ; S. Manzoor; A.U. Haq; M.A. Asgha ; W.A.G. Khawaja. Design and optimization of grid Integrated hybrid on-site energy generation system for rural area in AJK-Pakistan using HOMER software. AIMS Energy 2021, 9, 1113–1135.

[46] O. Guler , S.A. Akdag, Y.S. Cakir, 2013. Effects of data resolution on standalone hybrid system sizing. In: Renewable Energy Research and Applications International Conference on. IEEE, pp. 423–427, 2013.

[47] S. Jiang ; Z.A. Song. A review on the state of health estimation methods of lead-acid batteries. J. Power Sources 2022, 517, 230710.

[48] A. Bin, Y. Hongxing, H. Shen, L. Xianbo, 2003. Computer aided design for PV/Wind hybrid system. Renew. Energy 28, 1491–1512.

[49] M. Kharrich, O.H. Mohammed, N. Alshammari, M. Akherraz. Multi-objective optimization and the effect of the economic factors on the design of the Microgrid hybrid system. Sustainable Cities and Society 2021 ; 65 :102646.

[50] S. Mirjalili ; A. Lewis, A. Grey Wolf Optimizer. Adv. Eng. Softw. 2014, 69, 46–61.

[51] D. Guasch ; S. Silvestre. Dynamic Battery Model for Photovoltaic Applications. Prog. Photovolt. Res. Appl. 2003, 11, 193–206.

[52] M.M. Samy, S. Barakat Hybrid Invasive Weed Optimization – Particle Swarm Optimization Algorithm for Biomass/PV Micro-grid Power System 2019 Tanta University Egypt 1 6.

[53] Y. S. Mohammeda, B. B. Adetokun,O. Oghorada, Omotayo Oshiga, Techno-economic optimization of standalone hybrid power systems in context of intelligent computational multi-objective algorithms. Energy Reports 8 (2022) 11661–11674

[54] P. García-Triviño, F. Llorens-Iborra, C.A. García-Vázquez, A.J. Gil-Mena, L.M. Fernández Ramírez, F. Jurado. Long-term optimization based on PSO of a grid-connected renewable energy /battery /hydrogen hybrid system. Int J Hydrogen Energy 2014;39(21):10805–16.

[55] M. Kharrich, O.H. Mohammed, N. Alshammari, M. Akherraz. Multi-objective optimization and the effect of the economic factors on the design of the Microgrid hybrid system. Sustainable Cities and Society 2021 ; 65 :102646.